The Smallest Aromatic Tetracation Produced in Gas Phase by Intense Femtosecond Laser Pulses

Akihiro Kitashoji, Akimasa Fujihara, Taiki Yoshikawa, Tomoyuki Yatsuhashi

Akihiro Kitashoji, Akimasa Fujihara, Taiki Yoshikawa, Tomoyuki Yatsuhashi. (2019). The Smallest Aromatic Tetracation Produced in Gas Phase by Intense Femtosecond Laser Pulses. *Chemistry Letters*. 48, 1472-1475. doi:10.1246/cl.190667

The Smallest Aromatic Tetracation Produced in Gas Phase by Intense Femtosecond Laser Pulses

Akihiro Kitashoji,[1] Akimasa Fujihara,[2] Taiki Yoshikawa,[1] and Tomoyuki Yatsuhashi*[1]

[1] *Graduate School of Science, Osaka City University, 3-3-138, Sugimoto, Sumiyoshi-ku, Osaka 558-8585, Japan*
[2] *Graduate School of Science, Osaka Prefecture University, 1-1 Gakuen-cho, Naka-ku, Sakai, Osaka 599-8531, Japan*

E-mail: tomo@sci.osaka-cu.ac.jp

1 We report the production of the long-lived
2 hexafluorobenzene tetracation, which is the smallest
3 aromatic tetracation ever investigated, by 0.8 μm
4 femtosecond laser pulses. The tetracation yield relative to
5 that of trication radical is 0.11. Using the time-of-flight
6 mass spectrometer equipped with the fast ion gate and the
7 curved field reflectron, we estimate the lower limit of the
8 lifetime of tetracation to be 9 μs. Confinement of multiple
9 positive charges in a small organic molecule is unexpected;
10 however, our finding is an answer of this fundamental
11 concern.

12 Keywords: multiply charged ion, time-of-flight mass
13 spectrometry, tunnel ionization

14 Multiply charged ions are potentially different species
15 compared with cations, anions, and neutral radicals.
16 Macromolecules with several proton-accepting sites produce
17 multiply protonated molecules ($[M + nH]^{n+}$) by electrospray
18 ionization.[1] Matrix-assisted laser desorption/ionization also
19 forms multiply protonated molecules under specific
20 conditions.[2] Since multiply protonated molecules are stable
21 even-electron cations, fragmentation is initiated by
22 acquiring a certain activation energy. On the other hand, the
23 use of an intense femtosecond laser produces a different
24 form of multiply charged ions, such as multiply charged
25 molecular cations (MMCs, M^{z+}), by removing z electrons
26 via tunneling.[3] MMCs are unstable due to their
27 electron-deficient nature as well as strong Coulomb
28 repulsions within MMCs regardless of whether they are
29 formed as odd-electron cation radicals or even-electron
30 cations.[4] Therefore, intact MMCs have been little explored
31 to date although they have the potential to be a reactive
32 species due to their high electron affinity as well as high
33 potential energy.[5] In addition, investigations of intact
34 MMCs provide an opportunity to understand how
35 electron-deficient molecules maintain their chemical
36 bonding. In this study, we describe the production of the
37 smallest aromatic tetracation $C_6F_6^{4+}$ by femtosecond laser
38 pulses.
39 The experimental details have been described
40 elsewhere.[6] Gaseous C_6F_6 was ionized by focused linearly
41 polarized femtosecond laser pulses delivered from a
42 Ti:Sapphire laser (0.8 μm, 40 fs). The mass spectrum of
43 C_6F_6 (Figure 1a) taken by a Wiley−Mclaren time-of-flight
44 mass spectrometer (TOF-MS) with a linear configuration
45 (linTOF-MS) was dominated by MMCs ($C_6F_6^{z+}$, z =1−4),
46 which were definitively identified by their m/z and isotopic
47 structure. For example, a single peak appearing at m/z 46.5
48 and its accompanying single peak at m/z 46.75, shown in the
49 inset of Figure 1a, were assigned to those of $^{12}C_6F_6^{4+}$ and
50 $^{13}C^{12}C_5F_6^{4+}$, respectively. The peak area of $^{13}C^{12}C_5F_6^{4+}$

51 relative to that of $^{12}C_6F_6^{4+}$ was 0.070 (Figure S1), which is
52 close to the expected value (0.066) calculated by the isotope
53 abundance and chemical composition within the
54 experimental error.
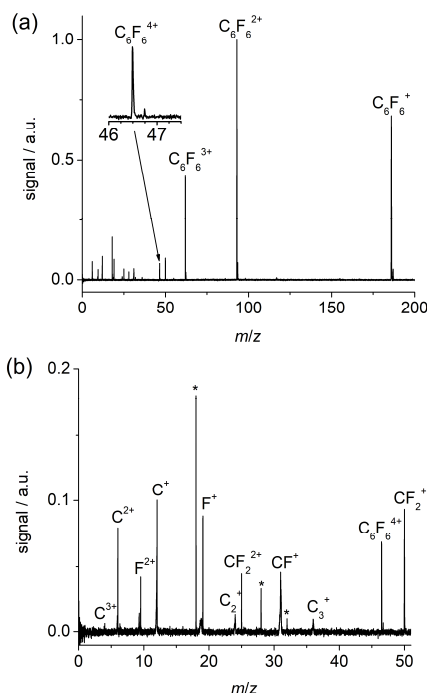
55

61 Figure 2a shows that the ion yield increased very
62 steeply as laser intensity increased until it reached the
63 saturation region. After reaching that region, the ion yield
64 stayed constant or decreased, depending on the balance
65 between the increase of ions by the volume effect and the
66 decrease of ions by the sequential ionization to a higher
67 charge state and/or fragmentation.[7] The appearance of
68 $C_6F_6^{z+}$ was evaluated by the saturation intensity,[8] which is
69 the index of ionization rate. Saturation intensity is defined
70 as the point at which the ion yield (linear scale),
71 extrapolated from the high-intensity linear portion of the
72 curve, intersects the intensity axis (logarithmic scale) as
73 shown in Figure 2b. Saturation intensities of $C_6F_6^{z+}$ were
74 1.1×10^{14} ($z = 1$), 1.2×10^{14} ($z = 2$), 2.1×10^{14} ($z = 3$), and
75 2.7×10^{14} W cm^{-2} ($z = 4$), respectively. The close proximity
76 of saturation intensities and similar laser intensity

dependences of MMC formation, despite their different ionization energies, leads us to conclude that sequential tunnel ionization processes rather than multiphoton ionization processes are operative in MMC productions.[9]

(a)

(b)

$C_6F_6^+$
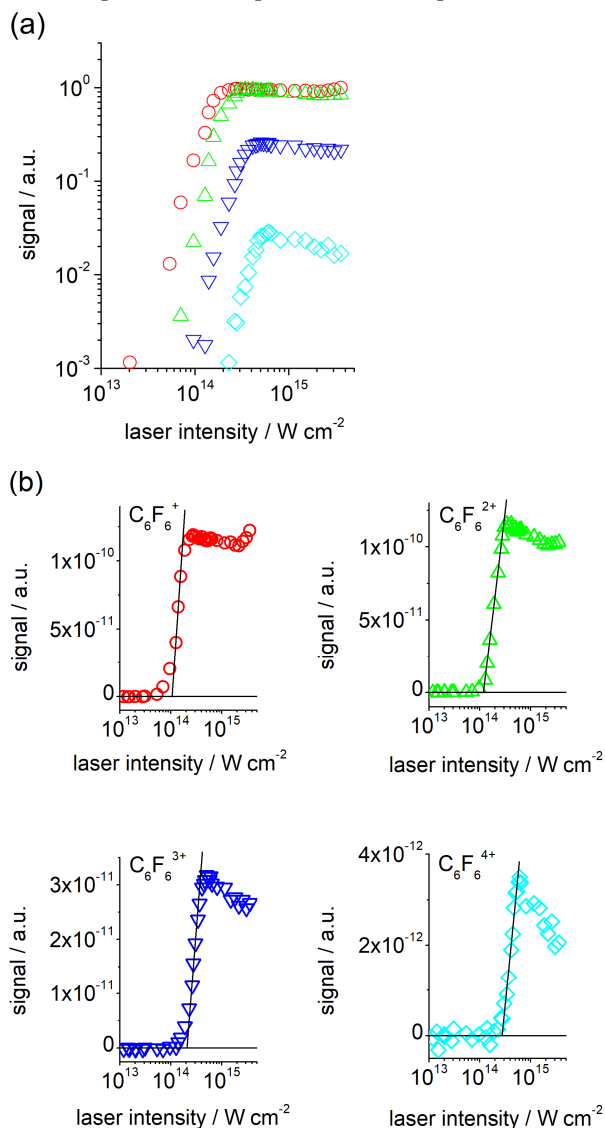
$C_6F_6^{2+}$

$C_6F_6^{3+}$

$C_6F_6^{4+}$

Figure 2. Ion signal of C_6F_6 as a function of laser intensity. (a) log-log plot and (b) semilog plot: $C_6F_6^+\cdot$ (circles); $C_6F_6^{2+}$ (triangles); $C_6F_6^{3+}\cdot$ (inverted triangles); $C_6F_6^{4+}$ (diamonds). The solid linear lines in (b) are the extrapolation from the high-intensity linear portion of the plots. The intersection with the intensity axis gives saturation intensity. The C_6F_6 pressure was 5×10^{-5} Pa.

The ratio of the peak area of $^{12}C_6F_6^{4+}$ relative to $^{12}C_6F_6^{3+}\cdot$ was largest (0.11) at 6.5×10^{14} W cm^{-2}. The ratio decreased as laser intensity increased (Figure S2), but the ratio was still large (0.077) even at the highest laser intensity (3.6×10^{15} W cm^{-2}). The formation of C_6F_6 tetracation in abundance is; however, somewhat surprising because Coulomb repulsion leading to dissociation is expected to dominate as the molecule shrinks.[5] Note that the maximum charge number of C_6H_6 found under the same laser irradiation condition was 3 (not shown), although C_6H_6 is more likely to be tetracation from an energetic point of view. The vertical ionization energies of C_6H_6 and C_6F_6 are 9.24 and 10.2 eV, respectively.[10,11] Since the ionization energies required for further ionization of the cation radical as well as of dication are proportional to the first ionization energy,[12] the multiple ionization of C_6H_6 is expected to be easier than that of C_6F_6 from an energetic standpoint. Therefore, the abundance of C_6F_6 tetracation owes to its stability, which in turn is due mainly to the absence of hydrogen atoms that are easily liberated as protons by Coulomb explosion. In 2011, the tetracation of the 4-atom molecule diiodoacetylene was found to be metastable due to the charge localization on the terminal iodine atoms.[13] Based on knowledge about the previously reported tetracations, it is necessary to ensure minimum Coulomb repulsion by maximizing the distance between charges, presumably with the aid of structural deformation,[14] in order to maintain the original chemical composition. High-level theoretical calculations using multi configurational method are required at least to understand how MMCs maintain their chemical bonding.[15] However, such calculations are great challenges and beyond the scope of the present work.

MMCs dominated the mass spectrum of C_6F_6, as shown in Figure 1a, but fragment ions (C_2^+, CF_2^{2+}, CF^+, C_3^+, CF_2^+, $C_5F_3^+$) and atomic ions (C^{3+}, C^{2+}, F^{2+}, C^+, F^+) were also detected by a linTOF-MS (Figures 1b). Most of these fragment and atomic ions are not originated from $C_6F_6^{z+}$ ($z = 1-4$), but from higher charge states of C_6F_6, which promptly dissociate by Coulomb explosion in the ion source.[16] Nevertheless, there might be concern that ions can dissociate on the time-scale of TOF detection by metastable ion decay (MID). However, linTOF-MS measurements cannot discriminate the ions formed by MID from that formed by prompt dissociation in the ion source. Once MID of an MMC occurs after leaving the ion source, related product ions are not accelerated in the drift (field-free) region of a TOF-MS. Therefore, the precursor MMC and its product ions have the same velocity and thus the same arrival time to the ion detector (MCP1 in Figure 3) in the case of the linTOF-MS configuration. In order to measure the product ions of specific precursor ion, we first select an ion packet including a precursor MMC and related product ions by a Bradbury-Nielsen ion gate (BNG), which alters the flight path of the unwanted ions to the detector.[17] The selected ion packet is further mass-separated by an offset curved field reflectron[18], which can focus the product ions with different kinetic energy to the detector. The product ions originating from the MID of a particular precursor MMC are then detected by the second ion detector (MCP2 in Figure 3). It should be mentioned that the m/z of measurable product ions is limited by that of the precursor ion.[19]

Figure 4 shows the product ion spectra of the selected MMC of $^{12}C_6F_6$. Spectra were taken under the elevated pressure of C_6F_6 (5×10^{-4} Pa) to improve the signal-to-noise ratio. As is clearly shown, product ions were not visible within the present signal-to-noise ratio range. This result

3

reveals that the noticeable MID of MMCs does not occur during the flight time in the drift region between the exit of the ion source and the entrance of the reflectron: 18 μs ($C_6F_6^{+\bullet}$), 13 μs ($C_6F_6^{2+}$), 10 μs ($C_6F_6^{3+\bullet}$), 9 μs ($C_6F_6^{4+}$).
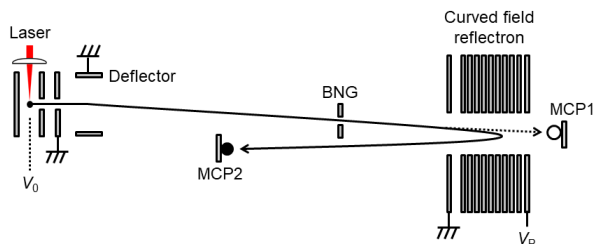
Figure 3. Schematic of TOF-MS (linTOF-MS, MCP1 is used, $V_R = 0$ V; refTOF-MS, MCP2 is used, $V_R = 3865$ V). V_0 is fixed to 2740 V.
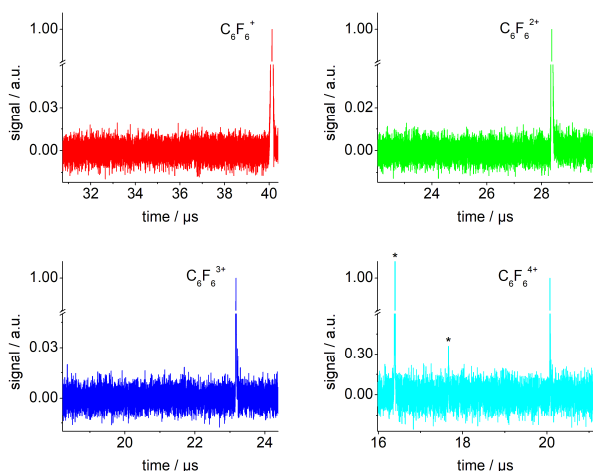
Figure 4. Time-of-flight spectra of particular $^{12}C_6F_6^{z+}$ measured by refTOF-MS (BNG was used, detected by MCP2, $V_R = 3865$ V). The pressure of C_6F_6 was 5×10^{-4} Pa. The laser intensity was 4.9×10^{14} W cm^{-2}. The spectral region where corresponding product ions appear is shown. * indicates the contaminated species (CF^+, C_3^+) formed in the ion source.

Here we compare the production of tetracations: the yield of tetracation relative to that of trication radical. The first detection of organic tetracation was done for ovalene ($C_{32}H_{14}$) in 1970 by electron ionization,[20] but ovalene tetracation was about 2 orders of magnitude less intense than the trication radical. In 1985, anthracene ($C_{14}H_{10}$) tetracation was produced by electron ionization, but its yield relative to the corresponding trication radical was quite small (7×10^{-6}).[21] In 2010, we showed the dramatic increase of the aromatic tetracation yield relative to that of trication radical by femtosecond laser pulses (1.4 μm, 130 fs):[22] 0.20 (triphenylene, $^{12}C_{18}H_{12}$), 0.08 (2,3-benzofluorene, $^{12}C_{17}H_{12}$). The maximum ratio to date (0.33 by 0.8 μm pulses) was obtained for octafluoronaphthalene ($C_{10}F_8$).[23] It should be mentioned that the number of aromatic tetracations reported to date is limited: 7 by electron ionization,[20,21] 3 by the collision with high-energy projectiles.[24] We have demonstrated the production of 4 aromatic tetracations including $C_6F_6^{4+}$,[22,23] but a systematic study, for example, a series of perfluoroaromatics, is necessary to show the trends about the production and stability of tetracations. Although the definitive conclusion cannot be made because the yield of MMCs is not only dependent on the ionization processes and thermodynamic stability but also photoreactivity, the charge delocalization over the aromatic moiety might determine the stability of tetracations based on the comparison between C_6F_6 and $C_{10}F_8$. Theoretical considerations about the electronic states of a series of perfluoroaromatic molecules are in progress.

References and Notes

1   Fenn, J. B.; Mann, M.; Meng, C. K.; Wong, S. F.; Whitehouse, C. M. *Science* **1989**, *246*, 64-71; McLuckey, S. A.; Stephenson, J. L. *Mass Spectrom. Rev.* **1998**, *17*, 369-407; Pitteri, S. J.; McLuckey, S. A. *Mass Spectrom. Rev.* **2005**, *24*, 931-958.

2   Koch, A.; Schnapp, A.; Soltwisch, J.; Dreisewerd, K. *Int. J. Mass Spectrom.* **2017**, *416*, 61-70; Cramer, R.; Pirkl, A.; Hillenkamp, F.; Dreisewerd, K. *Angew. Chem. Int. Ed.* **2013**, *52*, 2364-2367; McEwen, C. N.; Pagnotti, V. S.; Inutan, E. D.; Trimpin, S. *Anal. Chem.* **2010**, *82*, 9164-9168.

3   Ledingham, K. W. D.; Singhal, R. P.; Smith, D. J.; McCanny, T.; Graham, P.; Kilic, H. S.; Peng, W. X.; Wang, S. L.; Langley, A. J.; Taday, P. F.; Kosmidis, C. *J. Phys. Chem. A* **1998**, *102*, 3002-3005.

4   Nakashima, N.; Shimizu, S.; Yatsuhashi, T.; Sakabe, S.; Izawa, Y. *J. Photochem. Photobiol. C* **2000**, *1*, 131-143; Yatsuhashi, T.; Nakashima, N. *J. Photochem. Photobiol. C* **2018**, *34*, 52-84.

5   Mathur, D. *Phys. Rep.* **1993**, *225*, 193-272; Mathur, D. *Phys. Rep.* **2004**, *391*, 1-118; Schröder, D. *Angew. Chem. Int. Ed.* **2004**, *43*, 1329-1331; Schröder, D.; Schwarz, H. *J. Phys. Chem. A* **1999**, *103*, 7385-7394; Vekéy, K. *Mass Spectrom. Rev.* **1995**, *14*, 195-225.

6   Mitsubayashi, N.; Yatsuhashi, T.; Tanaka, H.; Furukawa, S.; Kozaki, M.; Okada, K.; Nakashima, N. *Int. J. Mass Spectrom.* **2016**, *403*, 43-52.

7   Yatsuhashi, T.; Obayashi, T.; Tanaka, M.; Murakami, M.; Nakashima, N. *J. Phys. Chem. A* **2006**, *110*, 7763-7771.

8   Hankin, S. M.; Villeneuve, D. M.; Corkum, P. B.; Rayner, D. M. *Phys. Rev. Lett.* **2000**, *84*, 5082-5085; Murakami, E.; Mizoguchi, R.; Yoshida, Y.; Kitashoji, A.; Nakashima, N.; Yatsuhashi, T. *J. Photochem. Photobiol. A* **2019**, *369*, 16-24.

9   Nagaya, K.; Mineo, H.; Mishima, K.; Villaeys, A. A.; Hayashi, M.; Lin, S. H. *Phys. Rev. A* **2007**, *75*, 013402.

10   Nemeth, G. I.; Selzle, H. L.; Schlag, E. W. *Chem. Phys. Lett.* **1993**, *215*, 151-155.

11   Bieri, G.; Asbrink, L.; Vonniessen, W. *J. Electron. Spectrosc. Relat. Phenom.* **1981**, *23*, 281-322.

12   Tobita, S.; Leach, S.; Jochims, H. W.; Ruhl, E.; Illenberger, E.; Baumgartel, H. *Can. J. Phys.* **1994**, *72*, 1060-1069; Yatsuhashi, T.; Nakashima, N. *J. Phys. Chem. A* **2005**, *109*, 9414-9418.

13   Yatsuhashi, T.; Mitsubayashi, N.; Itsukashi, M.; Kozaki, M.; Okada, K.; Nakashima, N. *ChemPhysChem* **2011**, *12*, 122-126;
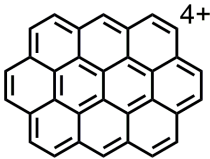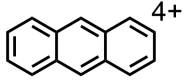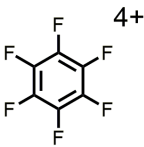
Yatsuhashi, T.; Toyota, K.; Mitsubayashi, N.; Kozaki, M.; Okada, K.; Nakashima, N. *ChemPhysChem* **2016,** *17*, 2977-2981.

14 Ibrahim, K.; Lablanquie, P.; Hubinfranskin, M. J.; Delwiche, J.; Furlan, M.; Nenner, I.; Hagan, D.; Eland, J. H. D. *J. Chem. Phys.* **1992,** *96*, 1931-1941.

15 Hammami, H.; Yazidi, O.; Rhouma, M. B.; Al Mogren, M. M.; Hochlaf, M. *J. Chem. Phys.* **2014,** *141*, 014302.

16 Shimizu, S.; Zhakhovskii, V.; Murakami, M.; Tanaka, M.; Yatsuhashi, T.; Okihara, S.; Nishihara, K.; Sakabe, S.; Izawa, Y.; Nakashima, N. *Chem. Phys. Lett.* **2005**, *404*, 379-383.

17 Kitashoji, A.; Yoshikawa, T.; Fujihara, A.; Kamamori, T.; Nashima, S.; Yatsuhashi, T. *ChemPhysChem* **2017,** *18*, 2007-2011.

18 Nikolaev, E. N.; Somogyi, A.; Smith, D. L.; Gu, C. G.; Wysocki, V. H.; Martin, C. D.; Samuelson, G. L. *Int. J. Mass Spectrom.* **2001**, *212*, 535-551; Satoh, T.; Sato, T.; Kubo, A.; Tamura, J. *J. Am. Soc. Mass. Spectrom.* **2011,** *22*, 797-803; Shimma, S.; Kubo, A.; Satoh, T.; Toyoda, M. *Plos One* **2012,** *7*, e37107.

19 Demirev, P. A.; Feldman, A. B.; Kowalski, P.; Lin, J. S. *Anal. Chem.* **2005,** *77*, 7455-7461; Liu, Z. L.; Schey, K. L. *J. Am. Soc. Mass. Spectrom.* **2008,** *19*, 231-238.

20 Bursey, M. M.; Rogerson, P. F.; Bursey, J. M. *Org. Mass Spectrom.* **1970,** *4*, 615-617.

21 Kingston, R. G.; Guilhaus, M.; Brenton, A. G.; Beynon, J. H. *Org. Mass Spectrom.* **1985,** *20*, 406-412.

22 Yatsuhashi, T.; Nakashima, N. *J. Phys. Chem. A* **2010,** *114*, 7445-7452.

23 Kitashoji, A.; Yatsuhashi, T. *Chem. Phys.* **2019**, *526*, 110465.

24 Ławicki, A.; Holm, A. I. S.; Rousseau, P.; Capron, M.; Maisonny, R.; Maclot, S.; Seitz, F.; Johansson, H. A. B.;. Rosén, S.; Schmidt, H. T.; Zettergren, H.; Mvanil, B.; Adoui, L.; Cederquist, H.; Huber, B. A. *Phys. Rev. A* **2011**, *83*, 022704; Rousseau, P.; Ławicki, A.; Holm, A. I. S.; Capron, M.; Maisonny, R.; Maclot, S.; Lattouf, E.; Johansson, H. A. B.; Seitz, F.; Mery, A.; Rangama, J.; Zettergren, H.; Rosen, S.; Schmidt, H. T.; Chesnel, J. Y.; Domaracka, A.; Manil, B.; Adoui, L.; Cederquist, H.; Huber, B. A. *Nucl. Instrum. Meth. B* **2012,** *279*, 140-143.

NOTE   *The diagram is acceptable in a colored form. Publication of the colored G.A. is free of charge.*
For publication, electronic data of the colored G.A. should be submitted. Preferred data format is EPS, PS, CDX, PPT, and TIFF.
If the data of your G.A. is "bit-mapped image" data (not "vector data"), note that its print-resolution should be 300 dpi.
You are requested to put a brief abstract (50-60words, one paragraph style) with the graphical abstract you provided, so that readers can easily understand what the graphic shows.

Graphical Abstract

Textual Information

A brief abstract (required)	The reports on the production of aromatic tetracations in gas phase have been limited to large molecules. Femtosecond laser irradiation to hexafluorobenzene results in the production of intact hexafluorobenzene tetracation that is the smallest aromatic tetracation ever reported. Negligible fragmetaion of this tetracation in microsecond time-scale is confirmed by using a time-of-flight mass spectrometer equipped with Bradbury-Nielsen ion gate and curved field reflectron.
Title(required)	The Smallest Aromatic Tetracation Produced in Gas Phase by Intense Femtosecond Laser Pulses
Authors' Names(required)	Akihiro Kitashoji, Akimasa Fujihara, Taiki Yoshikawa, and Tomoyuki Yatsuhashi

Graphical Information

The size is limited within 100 mm width and 30 mm height, or 48 mm square>(required)

46 atoms in 1970   24 atoms in 1985   12 atoms in this work